# Surface Selective ^{1}H and ^{27}Al MAS NMR Observations of Strontium Oxide Doped γ-Alumina

## Surface binding sites of strontium oxide on γ-alumina identified for the first time

**By Nathan S. Barrow\*, Andrew Scullard and Nicola Collis**

Johnson Matthey Technology Centre,
Blounts Court, Sonning Common, Reading,
RG4 9NH, UK

**Email:** nathan.barrow@matthey.com

High-surface area γ-alumina is industrially used as a catalyst support. Catalytically active elements are doped onto the support, where they can bind to $AlO_4$, $AlO_5$ or $AlO_6$ sites on the surface. Pretreating the surface with alkaline earth oxides can alter the availability of these surface sites, hence affecting the catalytic activity. The surface binding sites of strontium oxide (SrO) on γ-alumina were previously unknown. Direct [27]Al magic angle spinning nuclear magnetic resonance (MAS NMR) could not detect $AlO_5$ sites at 9.4 T, so [1]H–[27]Al cross-polarisation (CP) MAS NMR was used to preferentially select the surface environment signals. We directly observed the three surface environments on dehydrated γ-alumina as a function of SrO impregnation up to 4 wt% SrO. We found that $Sr^{2+}$ preferentially binds to $AlO_5$ and $AlO_6$ surface sites. ^{1}H MAS NMR revealed SrO impregnation causes a reduction in the terminal (−0.3 ppm) and bridging (2.2 ppm) hydroxyl environments, as well as the promotion of a new peak in between these sites, at 0.5 ppm. By using ^{1}H–^{27}Al CP/MAS NMR the relative proportions of surface sites on γ-alumina

can be determined, allowing an optimal level of SrO doping that can saturate all the $AlO_5$ sites. Importantly, this provides a method of subsequently depositing catalytically active elements on just the $AlO_4$ or $AlO_6$ sites, which can provide a different catalytic activity or stability compared to the $AlO_5$ binding site.

## 1. Introduction

Over 80 million tons of alumina are produced annually, which is used industrially for the production of aluminium and in applications requiring high melting point, excellent mechanical strength, electrical resistivity or chemical inertness (1). There are several polymorphs of alumina and the thermal transformations between them are well known (2). γ-Alumina in particular has a favourable combination of high surface area, pore size distribution and acid/base characteristics, which makes γ-alumina a common industrial catalyst support (3).

Specific applications of γ-alumina in catalysis include as a binder for zeolite catalysts in fluid catalytic cracking (4), as iron/copper/potassium (FeCuK) support for Fischer-Tropsch catalysis (5) and as a platinum support for dehydrogenation of jet fuel (6) or carbon monoxide oxidation (7). Three-way catalysts (TWC), which are widely used on gasoline engines to reduce CO, nitrogen oxides (NOx) and hydrocarbon emissions, include γ-alumina as part of the mixed oxide support because of its high surface area and relatively good thermal stability under hydrothermal conditions (8, 9). Barium oxide (BaO) and lanthana are commonly

used as stabilisers for alumina in TWC. An additional advantage of adding alkaline earth oxides to $\gamma$-alumina is the improvement of NOx storage for TWC (10, 11). Thus, the investigation of SrO structure on the surface of $\gamma$-alumina is one of practical importance. The matter is complicated as despite the massive production and industrial use of $\gamma$-alumina, the surface topography of $\gamma$-alumina is still under debate (12). Nevertheless, there is clear agreement that three main aluminium coordination environments exist on the surface: $AlO_4$, $AlO_5$ and $AlO_6$.

Solid-state nuclear magnetic resonance (SSNMR) of alumina is informative as the aluminium environments give distinct $^{27}Al$ peak positions; $AlO_4 \approx 60$ ppm, $AlO_5 \approx 30$ ppm and $AlO_6 \approx 0$ ppm. As $^{27}Al$ is a quadrupolar nucleus (13), the observed chemical shifts vary as a function of magnetic field strength, but remain distinct at all high fields (14). Studies on $\gamma$-alumina have been reported for the past 25 years, both using direct $^{27}Al$ NMR (15–17) as well as using $^{1}H$ to $^{27}Al$ CP NMR (12, 18, 19). More recently, dynamic nuclear polarisation (DNP) has been used to enhance the $^{27}Al$ NMR signals from the surface of $\gamma$-alumina, calculations have shown that the $^{27}Al$ CP signal is from the very first surface layer or primostrato (20, 21). This is in agreement with a deuteration experiment that concluded the CP signal does not come from interstitial or sub-surface hydrogens (18). Some computational studies disagree as the surface $^{27}Al$ nuclei are reported to have a large quadrupolar coupling, which broadens the $^{27}Al$ signal and makes CP ineffective (16, 22). However, the models used for these calculations did not account for surface rearrangement, which will favour less strained symmetric environments, as has been seen in alumina (23).

Penta-coordinated aluminium environments, i.e., $AlO_5$, exist on the surface of $\gamma$-alumina and can be observed using CP NMR (19, 21) or directly using high-field NMR measurements (24–27). Interestingly, little or no $AlO_5$ was observed by DNP NMR despite being a surface enhanced measurement, presumably because the alumina was mixed with an aqueous solution that reacted with the $AlO_5$ sites (20, 21). These $AlO_5$ sites have been shown to be the anchoring point for platinum oxide (26). Concerning alkaline earth oxide doping, $AlO_5$ has a one-to-one correlation against the number of BaO molecules impregnated on to $\gamma$-alumina (27). Hence, the surface $AlO_5$ sites are of great interest to the catalyst scientist.

Although no hydrogen atoms exist in the bulk of $\gamma$-alumina, the surfaces ({111}, {110} and {100})

are terminated by hydroxyl groups. Knözinger and Ratnasamy extended the earlier work of Peri who identified five types of hydroxyl environment on a hydroxylated ideal $\gamma$-alumina surface (28, 29). This model was again extended by Tsyganenko and Mardilovich who added a sixth environment, reproduced in **Figure 1**. (Note that in this article we refer to $Al_{IV}$ as $AlO_4$).

Many workers have reported $^{1}H$ NMR spectra of $\gamma$-alumina and attempted to assign peaks to specific hydroxyl environments. As-received $\gamma$-alumina contains a significant amount of physisorbed water throughout its porous structure, which overwhelms the $^{1}H$ NMR signal from the surface hydroxyls. Thus, all $^{1}H$ NMR experiments on $\gamma$-alumina must necessarily be performed after the sample has been heated above 250ºC to remove water and consequently the $\gamma$-alumina will be partially dehydroxylated. This is significant as penta-coordinated environments such as $OH^5$, $OH^{65}$ and $OH^{665}$, will be present that require assignment despite not having a particular Knözinger and Ratnasamy type (30–32). One limitation of this $^{1}H$ NMR technique is the requirement for drying, as the environments formed might not be present during, for example, a subsequent incipient wetness treatment to load the support with a catalytically active species.

Initial studies reported peaks of around −0.3 ppm, 2.4 ppm, 4.0 ppm and higher, which were assigned to the most basic OH group (type Ib), a more acidic group (type II), the most acidic (type III) and finally hydrogen-bonded protons, respectively (33, 34). Later studies appreciated the presence of $AlO_5$ with assignments of −0.2 ppm to −0.5 ppm: $OH^4$, 1.5 ppm to 2.5 ppm: $OH^{45}$,
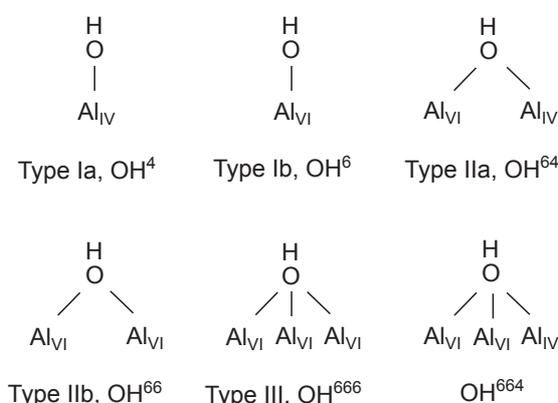


Fig. 1. Six surface hydroxyl environments that can exist on $\gamma$-alumina, labelled by Knözinger and Ratnasamy type and Tsyganenko and Mardilovich $OH^n$ nomenclature

2.5 ppm to 4.0 ppm: $OH^{nnn}$ and higher shifted hydrogen-bonded protons (12, 35, 36). These assignments are in agreement with the earlier studies, clearly showing the trend of increasing chemical shift going from terminal ($\mu^1$) to bridging ($\mu^2$) to $\mu^3$ OH environments.

To date, there have been no reports on the surface aluminium environments of any alumina that has been impregnated by SrO. The catalytic activity of a $\gamma$-alumina support, doped with an active species, will be affected by strontium doping that causes the surface environments to rearrange. For example, by blocking the $AlO_5$ sites, an active species can anchor to a weaker aluminium binding site ($AlO_4/AlO_6$), thus changing the catalytic activity. Accurate understanding of alkaline earth oxides on the surface of $\gamma$-alumina must explain changes in the aluminium coordination populations as well as $^1H$ NMR assignments. The scope of this article is to present novel NMR spectra on a strontium alumina system and suggest possible surface environments to explain those spectra. These hypotheses could be tested by future infrared measurements as well as *ab initio* calculations.

## 2. Experimental Results

1 wt%, 2 wt% and 4 wt% SrO on $\gamma$-alumina (Sasol) samples were prepared by incipient wetness impregnation using strontium nitrate (Alfa Aesar) dissolved in sufficient water. Following addition of the nitrate solution to the alumina, the samples were dried at 105ºC before being calcined at 500ºC for two hours.

Powdered samples were dried under vacuum at 350ºC overnight, before being packed in air-tight zirconia rotors under an inert atmosphere and were spun at 14 kHz in a static magnetic field strength of 9.4 T. A widebore Bruker 4 mm broadband (BB)/1H MAS probe was used. Spectra were normalised by mass and number of scans and all acquired on a Bruker Avance III console using TopSpin 3.1 software. All experiments used a 2 s recycle delay.

$^1H$ spectra were acquired (256 scans) with one rotor period spin echo experiment (37) and referenced to the low-ppm peak of adamantane-$d_{16}$ at 1.73 ppm. Pulse lengths were 3 µs (90º) and 6 µs (180º) at $v_{RF}$ = 83 kHz.

$^{27}Al$ spectra were referenced to yttrium-aluminium garnet (YAG) $AlO_6$ at 0.8 ppm (38). Direct acquisition (128 scans) used a 1.5 µs (<30º) pulse at $v_{RF}$ = 50 kHz. CP spectra (7168 scans) used a 1.5 ms contact pulse. $^{27}Al$ $v_{RF}$ = 12 kHz and $^1H$ $v_{RF}$ = 36 kHz to satisfy the Hartmann-Hahn condition (39, 40). The low

radio-frequency (RF) field gives selective spin-locking of the central transition ($m$ = ½ to −½), but under MAS, lineshapes will be distorted (41, 42). Proton decoupling did not improve resolution and was not used.

## 2.1 $^{27}Al$ Nuclear Magnetic Resonance

Directly acquired $^{27}Al$ spectra of the bulk are given in **Figure 2**. Peaks corresponding to $AlO_4$ and $AlO_6$ were clearly visible, present in an approximately 1:2 ratio by integration, which does not account for spinning sideband intensity. The contribution of surface $AlO_5$ environments was undetectably small against the background bulk signals. After normalising by sample mass, there was no significant variation in the bulk aluminium environments. This indicates that the SrO impregnation did not affect the structure of the $\gamma$-alumina nor form a strontium-aluminate phase.

Primostrato $^{27}Al$ CP spectra are given in **Figure 3**. Focusing initially on the undoped alumina; in contrast to the bulk spectra, the presence of $AlO_5$ was clearly visible. The ratio of $AlO_4$ and $AlO_6$ sites showed a preference for $AlO_6$ sites at the surface of $\gamma$-alumina. Although CP NMR spectra are not quantitative, the quadrupolar parameters of $AlO_4$ and $AlO_6$ were similar enough to allow for qualitative comparison. This is strong evidence that a surface rearrangement has taken place, i.e., the surface structure is not the same as the bulk structure.

The effects of SrO doping are also pronounced, with variation seen in all three types of aluminium environment. With the addition of 1% SrO there was an enhancement of $AlO_4$ signal, no change to the $AlO_5$ signal and a reduction in $AlO_6$ signal. For the $\gamma$-alumina with 2% SrO the $AlO_4$ signal was enhanced even more,
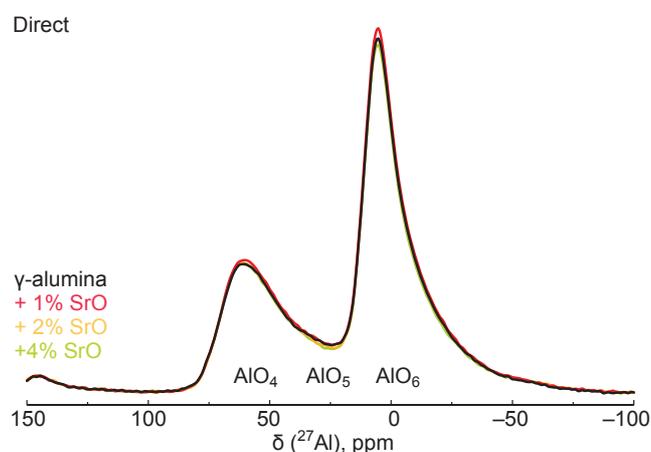


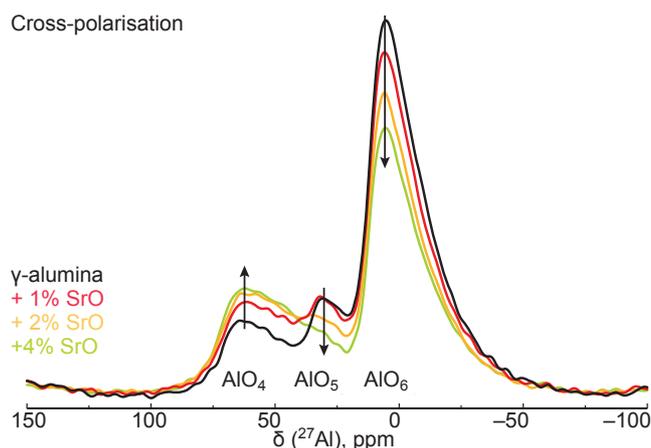Fig. 2. Normalised bulk $^{27}Al$ solid-state MAS NMR spectra

Fig. 3. Normalised primostrato $^{27}$Al solid-state CP/MAS NMR spectra

whilst there was a reduction in $AlO_5$ and $AlO_6$ signals. This trend continued for the 4% SrO sample.

Generally, a reduction in CP $^{27}$Al signal could be caused by several factors: (a) an actual physical reduction in that type of environment; (b) the removal of nearby hydrogen to that environment (as the magnetisation is transferred to aluminium from hydrogen) or (c) a distortion of the aluminium site symmetry causing extreme quadrupolar broadening and rendering the signal 'invisible'. The likelihood of these different factors occurring upon Sr doping will be discussed below.

## 2.2 $^1$H Nuclear Magnetic Resonance

The processed spectra are given in **Figure 4**. For the undoped γ-alumina three main environments were seen, in agreement with previous studies (12, 33, 35). These were assigned as HO-$\mu^1$ at −0.3 ppm, HO-$\mu^2$
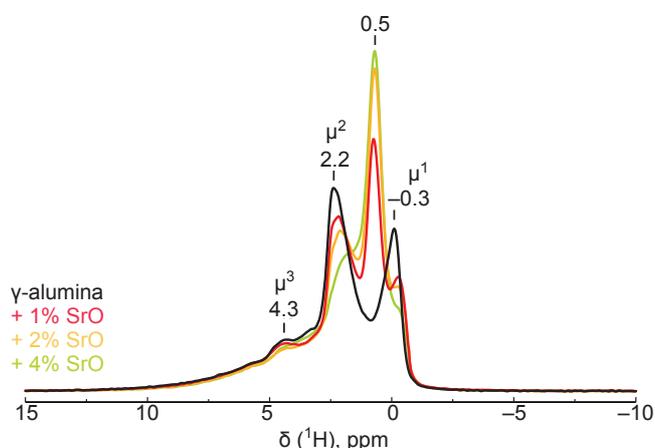
at 2.2 ppm and HO-$\mu^3$ at 4.3 ppm. Hydrogen-bonded environments also existed at higher chemical shifts, but in a lesser amount to the main environments.

Systematically doping γ-alumina with SrO produced an additional peak at 0.5 ppm whilst simultaneously reducing the terminal and bridging hydroxyl environments at −0.3 ppm and 2.2 ppm, respectively. The hydrogen-bonded and HO-$\mu^3$ environments appeared unaffected by the SrO doping.

As there are several specific types of surface hydroxyl group and the peaks appeared asymmetric, the spectra were deconvolved. At least seven peaks were required to obtain a good fit, although the lack of resolution meant that such a fit was ambiguous. Two of the fitted spectra are shown in **Figure 5**. The purpose of the fits is to show that a full structural model of the surface of γ-alumina must account for at least seven hydroxyl environments. Also, the fits show approximately how the various environments change upon doping with SrO.

Further experiments were performed to help assign the additional peak at 0.5 ppm. A strontium hydroxide ($Sr(OH)_2$) species was ruled out, as measurements on this material gave much higher chemical shifts. Both X-ray photoelectron spectroscopy (XPS) and chemical testing (addition of acid caused carbon dioxide evolution) indicated the presence of strontium carbonate ($SrCO_3$), which being energetically stable, is a likely surface species.

Hence, the 4% SrO γ-alumina sample was dosed with $CO_2$ overnight to promote a carbonate environment. The resulting $^1$H NMR spectrum is given in **Figure 6**. A loss



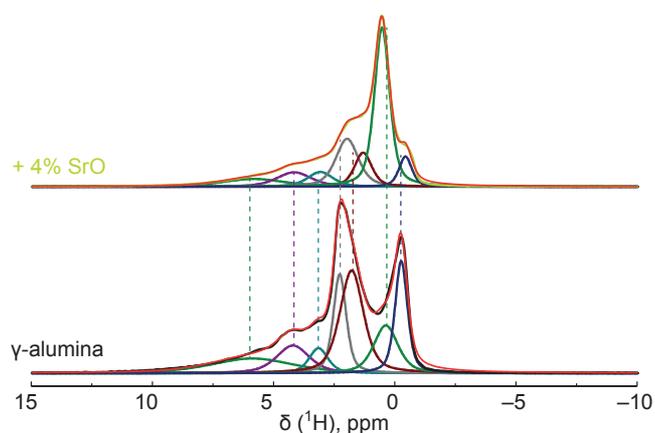Fig. 4. Normalised $^1$H solid-state MAS NMR spectra



Fig. 5. $^1$H solid-state MAS NMR spectra deconvoluted with seven half Gaussian, half Lorentzian peaks. Vertical dashed lines are a guide to the eye
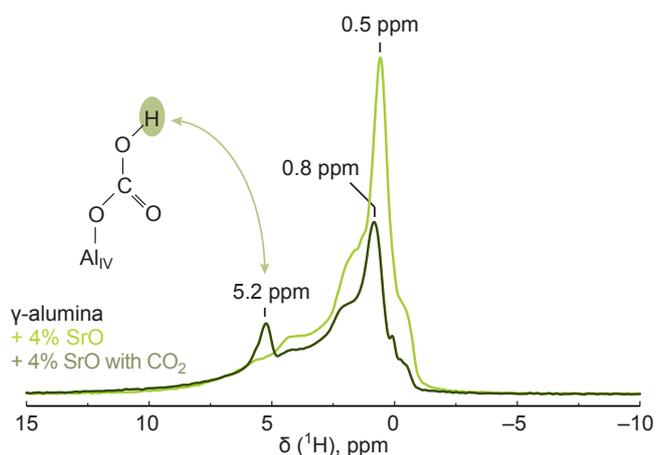
Fig. 6. Normalised $^1H$ solid-state MAS NMR spectra of $\gamma$-alumina doped with 4% SrO

of intensity for the HO-$\mu^1$ environment was observed and a new peak at 5.2 ppm was gained. This peak corresponds to an aluminium carbonate OH signal (12). Clearly the presence of Sr did not inhibit the adsorption of $CO_2$ on $\gamma$-alumina but significantly, this mechanism did not occur for atmospheric amounts of $CO_2$. This suggests the 0.5 ppm peak was not related to carbonate species.

In conclusion, SrO doping systematically affected the proton environments on $\gamma$-alumina, modifying the previously identified HO-$\mu^1$ and HO-$\mu^2$ hydroxyls and producing a new peak at 0.5 ppm. Although this new environment has not been identified, the correlation with SrO doping suggests the hydroxyls are proximate to some strontium compound, which will be discussed below.

## 3. Discussion

We first discuss the changes in the $^{27}Al$ CP/MAS NMR spectra upon SrO doping shown in **Figure 3**. The addition of SrO appears to preferentially replace the hydroxyls located at $AlO_5$ and $AlO_6$ sites. This preference could be because of the energetic favourability of $Sr^{2+}$ towards the more electronegative $AlO_5$ and $AlO_6$ sites. Consequently, the reduction in CP signal from the $AlO_5$ and $AlO_6$ sites is simply because of a reduction in nearby protons that the magnetisation would otherwise be transferred from. Whether Sr is present as isolated atoms or in SrO clusters is unclear from the $^{27}Al$ NMR.

An increase in $AlO_4$ CP signal upon SrO doping is harder to explain. One possibility for enhanced signal is to introduce additional hydroxyls. However, directly

bonded hydroxyls would increase coordination causing the signal to appear elsewhere, which has not been observed. Another possibility is that the presence of SrO promotes a structural rearrangement of higher coordination aluminium to $AlO_4$. This would be the opposite of condensation reactions typically seen when dopants are added to alumina and a plausible mechanism has not been forthcoming (43).

Two possibilities remain. One is that the addition of SrO causes $AlO_4$ sites to become more symmetric. This reduces their quadrupolar broadening giving rise to a more effective magnetisation transfer from $^1H$ to $^{27}Al$. Thus, previously 'invisible' $AlO_4$ sites appear in the primostrato spectra when SrO is added. Further experiments at multiple fields or using multiple quantum magic angle spinning (MQMAS) could be performed to determine the quadrupolar parameters and test this possibility. The other possibility is that SrO, replacing $AlO_5$ and $AlO_6$ hydroxyls, could then prohibit the fast exchange of protons across the surface, facilitating CP from the remaining protons on $AlO_4$ sites (16).

Next we discuss the changes in the $^1H$ spectra upon SrO doping shown in **Figure 4**. As mentioned above, the peak at 0.5 ppm grew in proportion with the quantity of SrO doped, which suggests these hydroxyls are proximate to some Sr compound. Additional experiments have ruled out the assignment of $Sr(OH)_2$ or $SrCO_3$. Furthermore, the chemical shift is in between the typical terminal and bridging environments. Combined with the unchanging environments above 4 ppm, these findings lead us to conclude that the peak at 0.5 ppm is from a shifted $OH^n$ or $OH^{nn}$ site.

As the most reactive/electronegative $OH^5$, $OH^6$, $OH^{56}$ and $OH^{66}$ environments have most likely been replaced by SrO, these are probably not an accurate assignment for the 0.5 ppm peak. The presence of an $OH^{44}$ environment is generally energetically unfavourable, so this too can be ruled out. This leaves us with modified $OH^4$ and/or $OH^{46}$ environments.

One issue with assignment is that the Sr form is currently unknown. $SrCO_3$, SrO clusters or $Sr^{2+}$ ions are possibilities. These three particular possibilities are shown in **Figure 7**, next to an $OH^4$ environment. As the deconvoluted proton spectrum in **Figure 5** suggested just one environment for the peak at 0.5 ppm, the likelihood is that just one of these mechanisms was present in our system.

Further evidence that favours the assignment of $OH^4$ comes from the $CO_2$ dosing results shown in **Figure 6**. As it has been shown that $CO_2$ preferentially goes
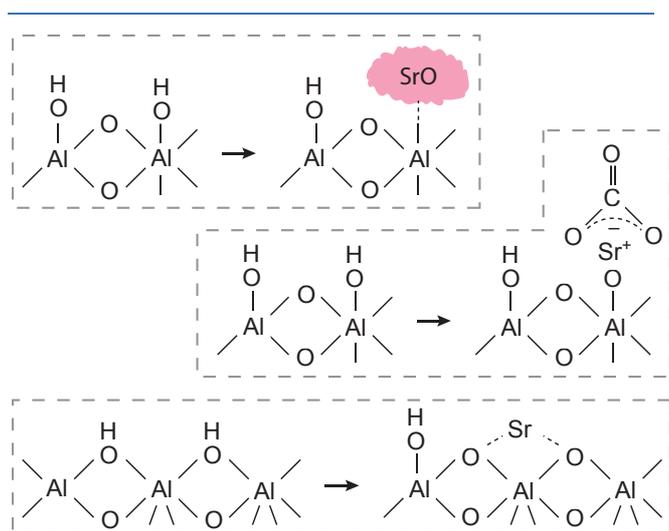
Fig. 7. Potential mechanisms whereby an OH[4] is modified by proximity to a SrO cluster, a strontium carbonate species and a Sr ion

to the OH[4] sites (12), the dramatic intensity loss of the 0.5 ppm peak strongly suggests this was a OH[4] environment.

## 4. Conclusion

The need for further research into the nature of the Sr environment and more comprehensive $^1$H peak assignments, is clearly indicated. This could be achieved through higher resolution $^1$H NMR experiments as well as $^1$H–$^{27}$Al correlation experiments. NMR data can be combined with infrared measurements to probe the hydroxyls. Raman microscopy and transmission electron microscopy (TEM) may also be used to elucidate the Sr environment. Ideally, the experimental data can all be used to create accurate surface models for density functional theory calculations to further explain the mechanisms at work in this system.

In conclusion, $^1$H–$^{27}$Al CP MAS NMR has shown that doping $\gamma$-alumina with SrO covers AlO$_5$ and alters the surface AlO$_4$:AlO$_6$ ratio. $^1$H MAS NMR revealed SrO impregnation caused a loss or shifting, of the terminal and bridging hydroxyl environments, with a new peak at 0.5 ppm hypothesised to be a modified OH[4] environment. These changes to surface chemistry will strongly affect where catalytically active metals are subsequently deposited. Such tunability for a common industrial catalyst support, like $\gamma$-alumina, is of great interest to the catalyst scientist.

## 5. Acknowledgements

## References

1. K. Wefers and C. Misra, "Oxides and Hydroxides of Aluminum", Alcoa Technical Paper No. 19, Aluminum Company of America, USA, 1987

2. G. Busca, 'Structural, Surface, and Catalytic Properties of Aluminas' in "Advances in Catalysis", ed. F. C. Jentoft, Volume 57, Academic Press, USA, 2014, pp. 319–404

3. M. Trueba and S. P. Trasatti, *Eur. J. Inorg. Chem.*, 2005, (17), 3393

4. J. S. J. Hargreaves and A. L. Munnoch, *Catal. Sci. Technol.*, 2013, **3**, (5), 1165

5. K. Keyvanloo, J. B. Horton, W. C. Hecker and M. D. Argyle, *Catal. Sci. Technol.*, 2014, **4**, (12), 4289

6. C. Lucarelli, S. Albonetti, A. Vaccari, C. Resini, G. Taillades, J. Roziere, K.-E. Liew, A. Ohnesorge, C. Wolff, I. Gabellini and D. Wails, *Catal. Today*, 2011, **175**, (1), 504

7. V. Novák, P. Kočí, M. Marek, F. Štěpánek, P. Blanco-García and G. Jones, *Catal. Today*, 2012, **188**, (1), 62

8. H.-Y. Chen and H.-L. Chang, *Johnson Matthey Technol. Rev.*, 2015, **59**, (1), 64

9. J. Kašpar, P. Fornasiero and N. Hickey, *Catal. Today*, 2003, **77**, (4), 419

10. C.-W. Yi, J. H. Kwak, C. H. F. Peden, C. Wang and J. Szanyi, *J. Phys. Chem. C*, 2007, **111**, (41), 14942

11. C. Verrier, J. H. Kwak, D. H. Kim, C. H. F. Peden and J. Szanyi, *Catal. Today*, 2008, **136**, (1–2), 121

12. M. Taoufik, K. C. Szeto, N. Merle, I. D. Rosal, L. Maron, J. Trébosc, G. Tricot, R. M. Gauvin and L. Delevoye, *Chem. Eur. J.*, 2014, **20**, (14), 4038

13. A. J. Vega, 'Quadrupolar Nuclei in Solids', in "eMagRes", ed. R. E. Wasylishen, John Wiley & Sons, Inc, Hoboken, New Jersey, USA, 2010

14. M. E. Smith and E. R. H. van Eck, *Prog. Nucl. Magn. Reson. Spectrosc.*, 1999, **34**, (2), 159

15. P. Nortier, P. Fourre, A. B. M. Saad, O. Saur and J. C. Lavalley, *Appl. Catal.*, 1990, **61**, (1), 141

16. B. A. Huggins and P. D. Ellis, *J. Am. Chem. Soc.*, 1992, **114**, (6), 2098

17. J. J. Fitzgerald, G. Piedra, S. F. Dec, M. Seger and G. E. Maciel, *J. Am. Chem. Soc.*, 1997, **119**, (33), 7832

18. H. D. Morris and P. D. Ellis, *J. Am. Chem. Soc.*, 1989, **111**, (16), 6045

19. D. Coster, A. L. Blumenfeld and J. J. Fripiat, *J. Phys. Chem.*, 1994, **98**, (24), 6201

20. V. Vitzthum, P. Miéville, D. Carnevale, M. A. Caporini, D. Gajan, C. Copéret, M. Lelli, A. Zagdoun, A. J. Rossini, A. Lesage, L. Emsley and G. Bodenhausen, *Chem. Commun.*, 2012, **48**, (14),1988

21. D. Lee, N. T. Duong, O. Lafon and G. De Paëpe, *J. Phys. Chem. C*, 2014, **118**, (43), 25065

22. R. Wischert, P. Florian, C. Copéret, D. Massiot and P. Sautet, *J. Phys. Chem. C*, 2014, **118**, (28), 15292

23. Y. Rozita, R. Brydson, T. P. Comyn, A. J. Scott, C. Hammond, A. Brown, S. Chauruka, A. Hassanpour, N. P. Young, A. I. Kirkland, H. Sawada and R. I. Smith, *ChemCatChem*, 2013, **5**, (9), 2695

24. R. Rinaldi, F. Y. Fujiwara, W. Hölderich and U. Schuchardt, *J. Catal.*, 2006, **244**, (1), 92

25. G. W. Wagner and R. A. Fry, *J. Phys. Chem. C*, 2009, **113**, (30), 13352

26. J. H. Kwak, J. Hu, D. Mei, C.-W. Yi, D. H. Kim, C. H. F. Peden, L. F. Allard and J. Szanyi, *Science*, 2009, **325**, (5948), 1670

27. J. H. Kwak, J. Z. Hu, D. H. Kim, J. Szanyi and C. H. F. Peden, *J. Catal.*, 2007, **251**, (1), 189

28. J. B. Peri, *J. Phys. Chem.*,1965, **69**, (1), 220

29. H. Knözinger and P. Ratnasamy, *Catal. Rev.: Sci. Eng.*, 1978, **17**, (1), 31

30. A. A. Tsyganenko and P. P. Mardilovich, *J. Chem. Soc., Faraday Trans.*, 1996, **92**, (23), 4843

31. M. Digne, P. Sautet, P. Raybaud, P. Euzen and H. Toulhoat, *J. Catal.*, 2004, **226**, (1), 54

32. A. R. Ferreira, E. Küçükbenli, S. de Gironcoli, W. F. Souza, S. S. X. Chiaro, E. Konstantinova and A. A. Leitão, *Chem. Phys.*, 2013, **423**, 62

33. E. C. Decanio, J. C. Edwards and J. W. Bruno, *J. Catal.*, 1994, **148**, (1), 76

34. F. Deng, G. Wang, Y. Du, C. Ye, Y. Kong and X. Li, *Solid State Nucl. Magn. Reson.*, 1997, **7**, (4), 281

35. M. Delgado, F. Delbecq, C. C. Santini, F. Lefebvre, S. Norsic, P. Putaj, P. Sautet and J.-M. Basset, *J. Phys. Chem. C*, 2012, **116**, (1), 834

36. N. Huittinen, P. Sarv and J. Lehto, *J. Colloid Interface Sci.*, 2011, **361**, (1), 252

37. E. L. Hahn and D. E. Maxwell, *Phys. Rev.*, 1951, **84**, (6), 1246

38. D. Massiot, C. Bessada, J. P. Coutures and F. Taulelle, *J. Magn. Reson.*, 1990, **90**, (2), 231

39. S. R. Hartmann and E. L. Hahn, *Phys. Rev.*, 1962, **128**, (5), 2042

40. A. J. Vega, *J. Magn. Reson.*, 1992, **96**, (1), 50

41. S. Hayashi, *Solid State Nucl. Magn. Reson.*, 1994, **3**, (2), 93

42. S. E. Ashbrook and S. Wimperis, *J. Chem. Phys.*, 2004, **120**, (6), 2719

43. P. J. Chupas and C. P. Grey, *J. Catal.*, 2004, **224**, (1), 69

## The Authors

Nathan Barrow is currently a Principal Scientist in the Advanced Characterisation department at the Johnson Matthey Technology Centre, Sonning Common, UK. He graduated with an MPhys in 2006 from the University of Warwick, UK, where he remained to gain a PhD in SSNMR. In 2010 Barrow was a Knowledge Transfer Partnership associate between the University of Warwick and Johnson Matthey, helping to install and run an SSNMR service. His current research focuses on applying advanced characterisation to materials such as zeolites, alumina, glasses and batteries.

Andrew Scullard joined Johnson Matthey in 2006 upon graduation from the University of Surrey, UK, where he studied Chemistry with Business. As part of this course he spent a year working in the pharmaceuticals industry for Eli Lilly. Since joining Johnson Matthey he has spent the majority of his time in the Low Carbon Technology Group working on customer funded and EU funded projects focused on greenhouse gas abatement, reforming and sulfur removal.



After graduating from the University of Southampton, UK, Nicola Collis joined Johnson Matthey working on catalyst preparation for fuel cells where she looked at generating robust metal alloy particles for proton exchange membrane fuel cell applications. Nicola subsequently transferred to emission control research where she specialises in metal solution chemistry and support surface chemistry, focusing on how to design catalyst particles and control metal-support interactions during catalyst preparation.